

Characterization Of Black Phosphorous Synthesized Via Ball-Milling Technique for The Effect of Milling Media and Time

Zainul Abidin Lukman¹, Irwan Nurdin², Mohd Shahadan Mohd Suan^{1,*}

¹ Fakulti Teknologi dan Kejuruteraan Industri dan Pembuatan, Universiti Teknikal Malaysia Melaka, 76100 Durian Tunggal, Melaka, Malaysia

² Chemical Engineering Department, Lhokseumawe State Polytechnic, 24301 Aceh, Indonesia

ARTICLE INFO

Article history:

Received 23 January 2024

Received in revised form 19 February 2024

Accepted 27 March 2024

Available online 30 April 2024

Keywords:

Black phosphorus; ball-milling technique; milling parameters

ABSTRACT

Black phosphorus (BP), a unique arm-chair structure 2D material named for its distinctive black colour has been known to have intriguing properties include high energy storage and energy band-gap capabilities. BP is synthesized from the red phosphorus by using the ball-milling technique as an alternative to the existing complicated method which involves hazardous white phosphorus, high-temperature, and high-pressure conditions. Hence, we investigated and compared the effects of using alumina, stainless steel, and agate media on BP's physical and structural properties. The effects of milling time were performed afterward by using stainless-steel media for 1 h to 5 h. The ball-milling process at 450 rpm for 5 h in stainless steel media has transformed the coarse red powder into a dark black colour fine powder. The XRD analysis on the as-prepared powder revealed the existence of pure and crystalline black phosphorus. The Raman analysis indicated the apparent existence of BP structure synthesized. Observation of the FESEM images showed the BP existed with nanosized and flaky-shaped microstructure.

1. Introduction

Black phosphorus (BP) is the most stable allotrope of phosphorus element and has been reintroduced recently due to its energy storage capability for high-efficiency, high-capacity, and fast charge/discharge rate of battery and supercapacitor. Like graphene and transition metal dichalcogenides (TMDs), BP has a monoatomic heterostructure layer but with a unique puckered single-layer geometry [1,2]. However, the difficulties to synthesize large quantities of BP is a major concern to its advancement. Synthesis of BP mostly involves the highly reactive white phosphorus as the raw material while the red phosphorus (RP) needs a complex method and demands high-pressure-temperature environments to be transformed into BP [3]. Ball milling is a process that uses mechanical energy to synthesize nanostructures [4,5]. The interaction of the milled material with the balls and with the vessel wall results in immediate high temperatures and high pressures, which can lead to significant phase changes [6]. The ball-milling technique can be an efficient way to synthesize

* Corresponding author.

E-mail address: mohdshahadan@utem.edu.my

<https://doi.org/10.37934/armne.18.1.113122>

BP because this method could generate high temperature and pressure due to collisions, friction, and shear between milling material and medias.

In 2007, Park and Sohn [4] demonstrated the production of (BP) using a high energy mechanical milling (HEMM) process at atmospheric pressure and temperature. The process involves the mechanical grinding of precursor materials in the presence of a milling medium. To convert red phosphorus into BP, the temperature and pressure must be high. The local pressures and temperature can be about 6 GPa, and as high as 200 °C, during the process of HEMM, which is sufficient for the conversion to take place [5]. Therefore, the milling media and time play important roles in ensuring sufficient temperature and impact can be obtained and sustained. Wide selection of milling media had been used include stainless steel, alumina, agate, zirconium oxide, and tungsten carbide [7-9]. Chenje *et al.*, [10] suggested that the selection of the milling media was varied by different types of compounds and the required properties. Meanwhile, there were wide range of milling time has been used starting from 1 hour up to 12 hours that resulted with various phase of BP from semi-crystalline and highly crystalline structure of BP [11,12]. The clear detail on the most effective milling media and time towards the BP transformation however still unspecified. Thus, this work investigates the effects of using alumina, stainless steel, and, agate media together with the milling time on the structural properties of synthesized BP powder.

2. Methodology

High-purity RP powder (Sigma Aldrich) has been used as the starting material to obtain BP. The powder was weighted and transferred into the milling jar containing a determined number of milling balls. Each RP handling process was performed in a glove box to sustain the stabilities of RP powder. There were 3 types of milling media (jar and balls) used; alumina, agate and stainless steel as shown in Figure 1. The jar was carefully sealed to avoid air infiltration. The ball-milling process was performed using a PM 100 planetary ball mill machine (Retsch, Germany). The machine was programmed to maintained a rotation speed of 450 rpm at a maximum time of 8 h. Afterwards, by using the selected media (based on results from various media), the process was repeated at 1 h, 2h, 3 h, 4 h and 5 h to investigate the most efficient milling time for the BP phase transformation.



Fig. 1. Milling media (a) Agate (b) Stainless steel (c) Alumina

The resultant powders were physically observed by using a light microscope. Further structural, bonding, and microstructural characterizations of the powder were completed by using X-ray diffraction (XRD, Rigaku Miniflex) with Cu K α radiation from 10-90° scanning angle, Raman

Spectroscopy (UniRAM) with 532 nm excitation laser and FESEM (Hitachi Scottky SU5000) with 500,000 x magnification respectively.

3. Results and Discussions

3.1 Effects of The Milling Media

The physical observation of the as-prepared powders revealed color changes due to the existence of BP. Figure 2 shows the red color of RP has been obviously changed into various tones of black powder after the ball-milling process. The as-prepared powder in agate media appeared greyish black compared to the other dark black samples. The dark black color of the powder may indicate a complete and uniform transformation from RP into BP as discussed by Bao *et al.*, [11]. The high pressure and temperature during the milling process promote the changes of color of RP in all the media as demonstrated by previous research [12,13]. Further, the powder produced in stainless steel and alumina media existed in finer sizes. Stainless steel and aluminum media's high hardness leads to more effective breakage of larger particles into smaller ones, leading to a finer powder size distribution [14,15]. As for agate, due to its lower hardness compared to stainless steel and alumina, it is less effective in breaking down larger particles.

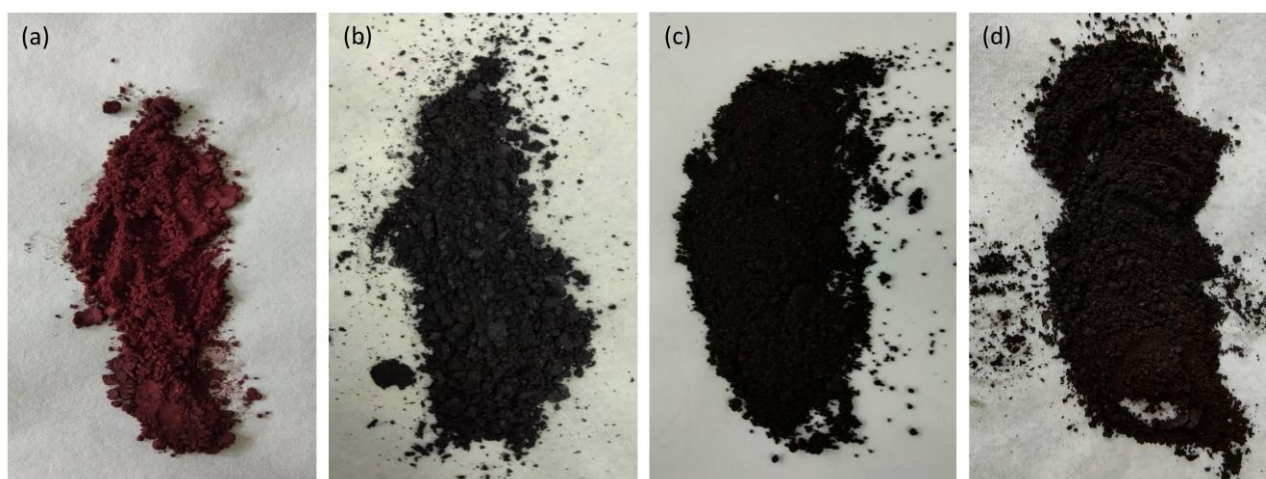


Fig. 2. Physical appearance of RP powder and as-prepared BP powders after the ball-milling process at 450 rpm for 8 h using various media; (a) RP, (b) agate, (c) stainless-steel, and (d) alumina

Figure 3 shows the XRD patterns spectra of the RP and the as-prepared powders. The most significant XRD peak attributed to BP by (040) plane diffraction has occurred in each milled powder suggesting the existence of crystalline BP. The (040) plane is a subset of the crystallographic planes in the BP lattice which indicates that milled powder has crystallinity [16-18]. Further analysis revealed a complete transformation of RP into BP occurred in the samples from alumina and stainless-steel media signified by peaks from (060), and (020) planes. However, there were impurity peaks detected on alumina XRD patterns that maybe due to incomplete transformation of RP into BP. The transformation happens when pressure or temperature is applied to the RP sample causing the atoms in the crystal lattice to rearrange. The alumina and the stainless-steel media put enough pressure on the red phosphorus sample to cause the transformation. The complete formation of crystalline BP structure by stainless-steel media corresponds well with the previous XRD study [19].

Figure 4 shows the Raman spectra for the RP and BP powders. The expected BP vibrational modes around 340, 430, and 460 cm^{-1} respectively [20] were observed for samples milled using alumina and stainless-steel media. The slightly raised background between 500 to 550 cm^{-1} is likely attributed to

residual Al for the sample synthesized in the alumina media. The aluminum species in the sample that's been synthesized in the alumina media can give off an extra signal in this part of the spectrum. Aluminum has its own Raman peaks that are usually seen in the range of $400 - 500 \text{ cm}^{-1}$, and these peaks can overlap or add to the background in the range of $500 - 550 \text{ cm}^{-1}$, giving off a slightly higher background in the spectrum [21,22].

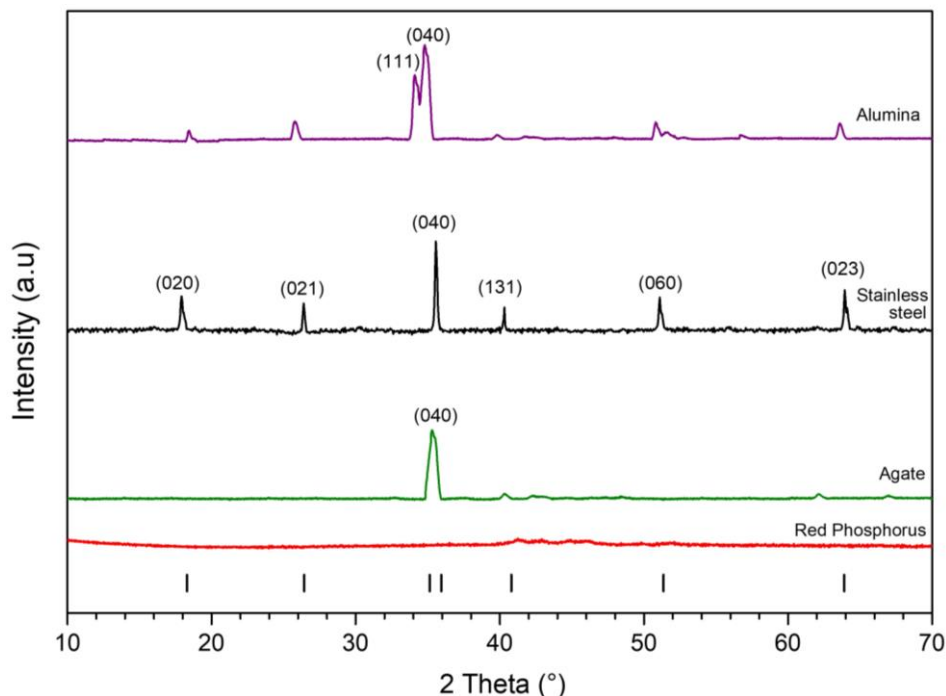


Fig. 3. XRD patterns of RP powder and as-prepared BP powders after ball-milling process at 450 rpm for 8 h using various milling media. Bars at bottom indicated Bragg diffraction pattern for BP

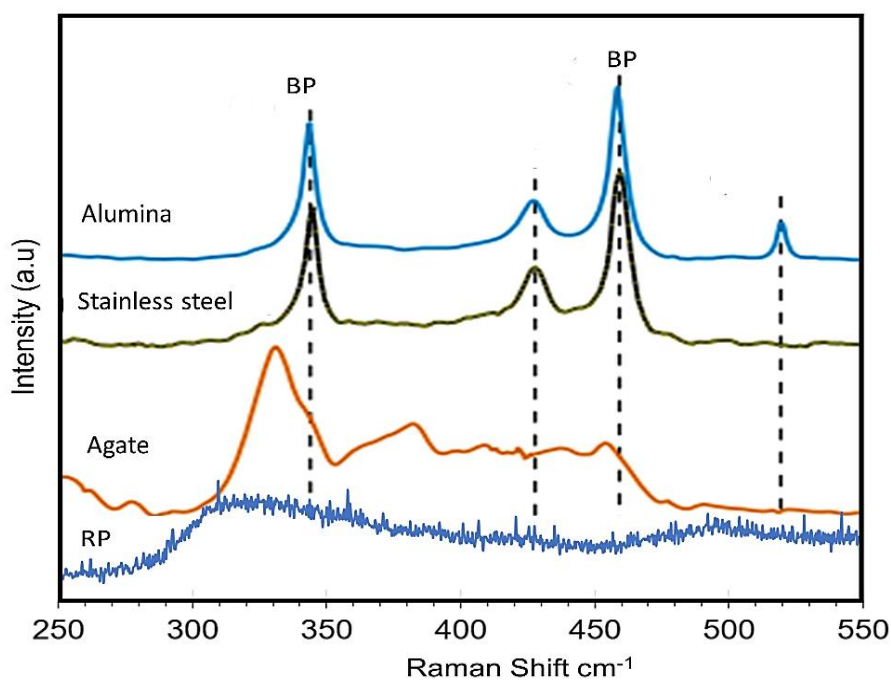


Fig. 4. Raman Spectra of RP powder and as-prepared BP powders after the ball-milling process at 450 rpm for 8 h using various milling media

Complete structural transformation of RP into BP was reported to occur at temperature $>800\text{ }^{\circ}\text{C}$ and $\approx 25\text{ mJ}$ impact energy [8]. It can be suggested that the capability of the alumina and stainless-steel media to achieve both conditions have resulted in the complete transformation of BP. When the media particles collide with red phosphorus, they heat up the areas they encounter. This heating causes the temperature to rise in those areas, which is what sets the stage for the transformation. The friction between the particles and the red phosphorous structure also creates mechanical pressure that helps break up the bonds in the red phosphorous structure and allows the atoms to be rearranged into the black phosphorous lattice.

Microstructures of RP and BP powders are shown in the Figure 5. RP existed as particulate microstructure ($\sim 0.1\mu\text{m}$) which agglomerated into bulky grains as depicted in Figure 5(a) while the BP in Figure 5(b), (c) and (d) shown flaky microstructures ($0.05\text{-}0.1\mu\text{m}$) respectively.

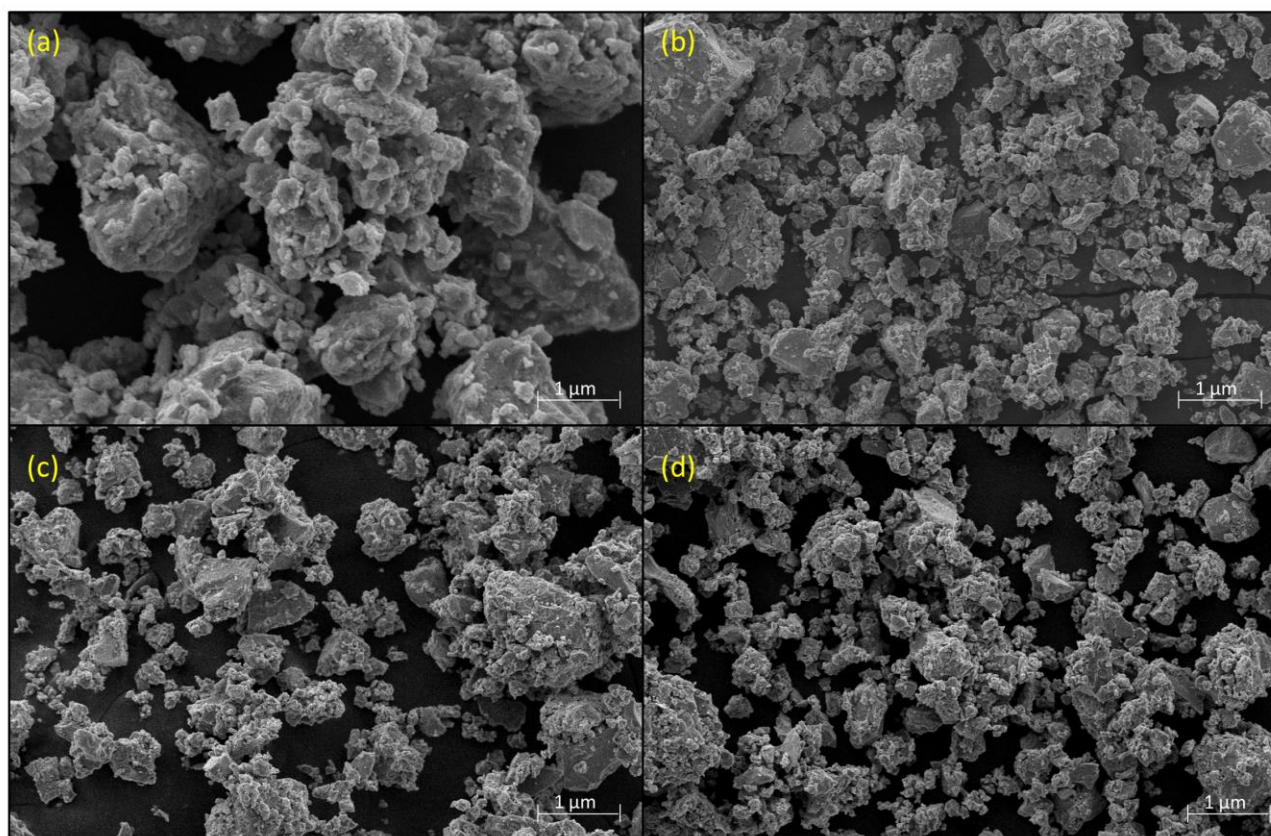


Fig. 5. FESEM images at 50,000 x magnifications of RP powder and as-prepared BP powders after the ball-milling process using various milling media; (a) RP, (b) agate, (c) stainless-steel, and (d) alumina

As the bulk RP powder undergoes the milling process, the RP receives high impact and shear force between media collisions where the particle size is reduced and the specific surface area. The flaky structure of BP is the evidence of BP occurrence as suggested by Kou *et al.*, [23]. BP appeared with flaky microstructure as the result of stacks of multilayers of 2D phosphorene [24,25]. The flaky microscopic structure of BP is derived from the layered crystal structure of BP. Each layer of BP is composed of a 2D sheet of phosphorous atoms, arranged in a lattice structure analogous to the honeycomb structure of graphene. The sheets of BP are deposited on top of one another by weak Van der Waals force, resulting in the bulk structure.

3.2 Effects of The Milling Time

Figure 6 shows the physical appearance of the RP and BP powders after being milled at various times. It can be seen that the colour appearance of the red powder was significantly changes with milling times. After 1 h of milling, the powder colour appears to exhibit a brownish-red colour with some black powder mix as it indicates the formation of BP crystal. From 2 h onward the colour appears to turn completely black and gets darker as the milling time increases. At 5 h, the RP turned completely into a dark black colour. This indicates, as the BP crystal formation content rises, the RP powder's colour visually shifts from a burned umber red to a dark black with various shades of red, brown, and black.

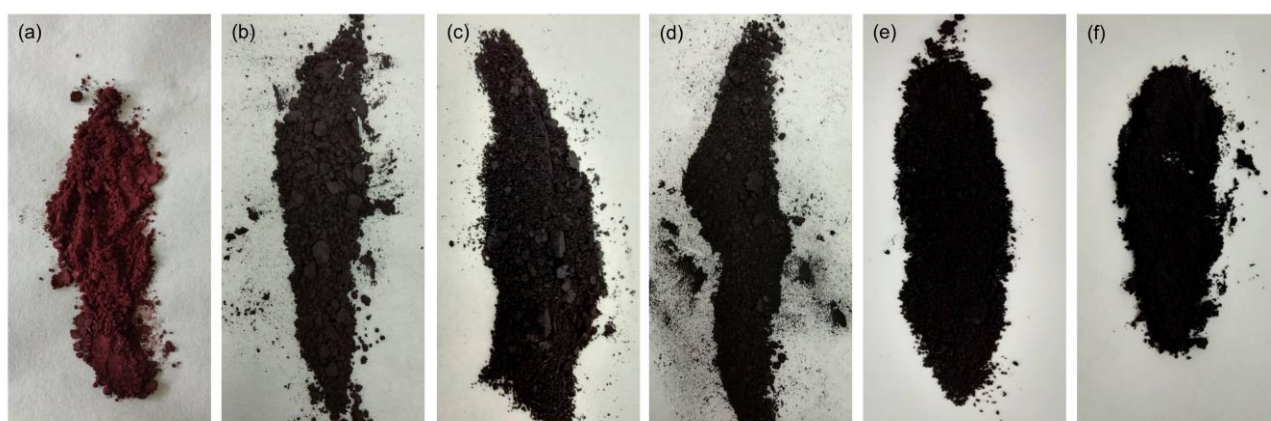


Fig. 6. Physical appearance of RP powder and as-prepared BP powders after the ball-milling process using stainless-steel media at 450 rpm varied by milling time; (a) 0 min, (b) 1 h, (c) 2 h, (d) 3 h, (e) 4 h and (f) 5 h

Figure 7 shows the XRD patterns for RP and BP after different milling times. Comparing the RP pattern to the BP patterns, the results demonstrated that the crystalline structure of BP has been transformed successfully through the milling process. The amorphous structure of RP shown by a broad XRD curve in Figure 6 was slowly transformed into BP crystalline structure by the existence of XRD sharp peaks on the curve. The most significant BP diffraction peak (020), (040) and (060) start appearing at 1 h and became apparent at 3 h. These peaks getting intense as the milling time was increase to 4 h. Full transformation of RP into BP only occurred after 5 h of milling process indicated by highly intense of BP diffraction pattern and elimination of the impurity peaks. The pattern for 5 h sample is similar to the 8 h sample discussed in part 3.1 which is in agreement with the other studies [26,27]. The lattice constants which indicate the geometry of the crystal cell obtained from the (040) peak is shown in Table 1 and confirmed the orthorhombic structure of BP.

Table 1
 Lattice constants change with milling times

Milling Time (h)	a (Å)	b(Å)	c(Å)	Orthorhombicity
1	3.283	10.415	4.389	0.521
2	3.267	10.520	4.389	0.526
3	3.374	10.707	4.313	0.521
4	3.375	10.389	4.313	0.510
5	3.379	10.389	4.313	0.509

As shown in the Figure 7, the BP shows 3 significant peaks starting from 2 h to 5 h milling times. The XRD results matched well with the standard pattern of BP crystal structure. Wang *et al.*, 2018

state that the milling time plays a very important role in the phase transformation from RP to crystalline BP in the ball milling process [28]. Increase in milling times result in a longer collision frequency rate between the powder, balls and jar resulting in higher BP crystal formation. In the other hand, further increase of milling time would consume more energy. Based on the XRD results, transformation of highly pure and crystalline BP can be obtained after 5 h of milling.

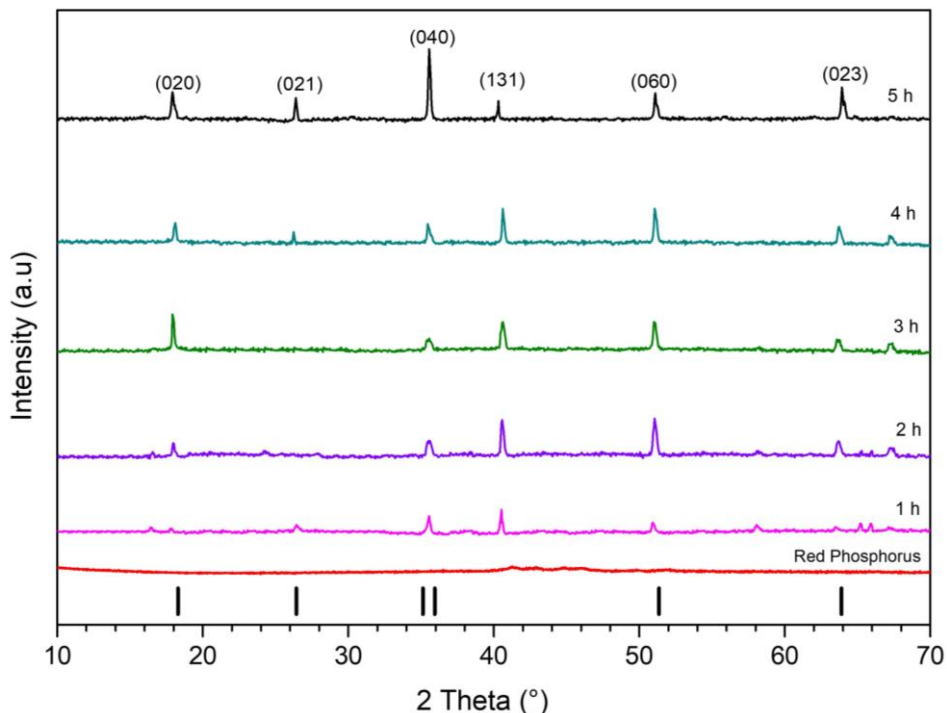


Fig. 7. XRD patterns of RP powder and as-prepared BP powders after the ball-milling process using stainless-steel media at 450 rpm at various milling time. Bars at bottom indicated Bragg diffraction pattern for BP

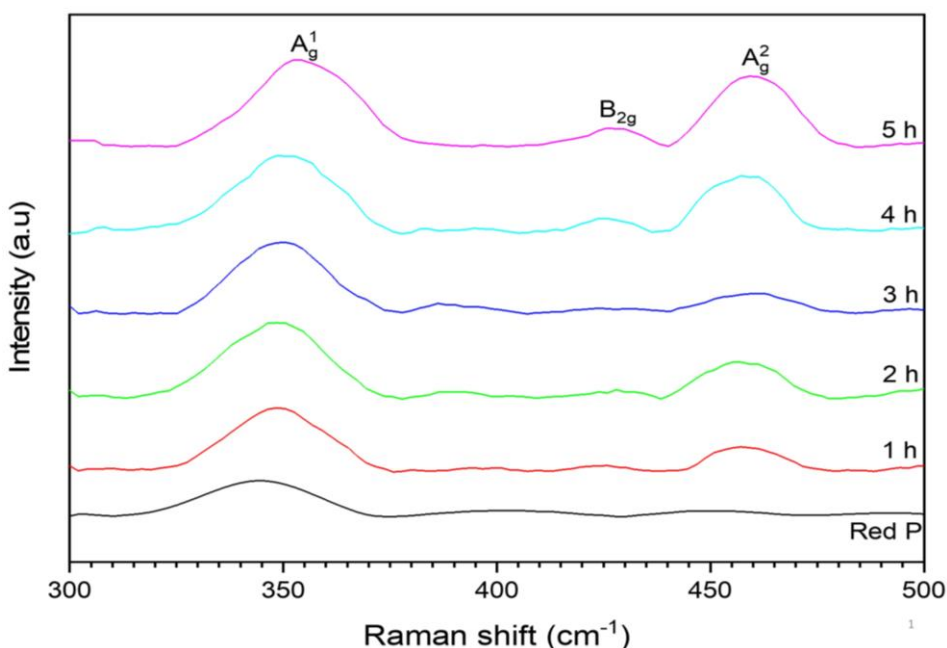


Fig. 8. Raman Spectra of RP powder and as-prepared BP powders after the ball-milling process using stainless-steel media at 450 rpm at various milling time

Raman spectroscopy pattern for RP and BP powders sample varied by different milling times. are shown in Figure 8 Based on the results, starting from 4 h and get intense after 5 h of milling times, three Raman peaks that can be observed at $\approx 361.0\text{ cm}^{-1}$, $\approx 432.0\text{ cm}^{-1}$, and $\approx 465.0\text{ cm}^{-1}$ corresponding to the A^1_g , B^2_g , and A^2_g modes, respectively. The peaks were assigned to BP and match well with other reports [26,29]. The Raman pattern in Figure 8 revealed fully transformation of RP into BP after 5 h of milling which aligned to XRD results.

Figure 9 shows the FESEM images of RP and BP powder. It can be observed the RP starting powder has an irregular faceted microstructure. It can be observed that fine BP particles were existed along the RP microstructure in Figure 9 (b), (c) and (d) after the milling process went through 1h, 2 h, and 3 h respectively. Further increase of milling time resulted to replacement of RP microstructure by BP particles as shown in Figure 9 (e) and (f). Close observations revealed that the BP particles existed as aggregates flakes of crystalline domains. As revealed in section 3.1, The flaky microscopic structure of BP is derived from the layered crystal structure of BP.

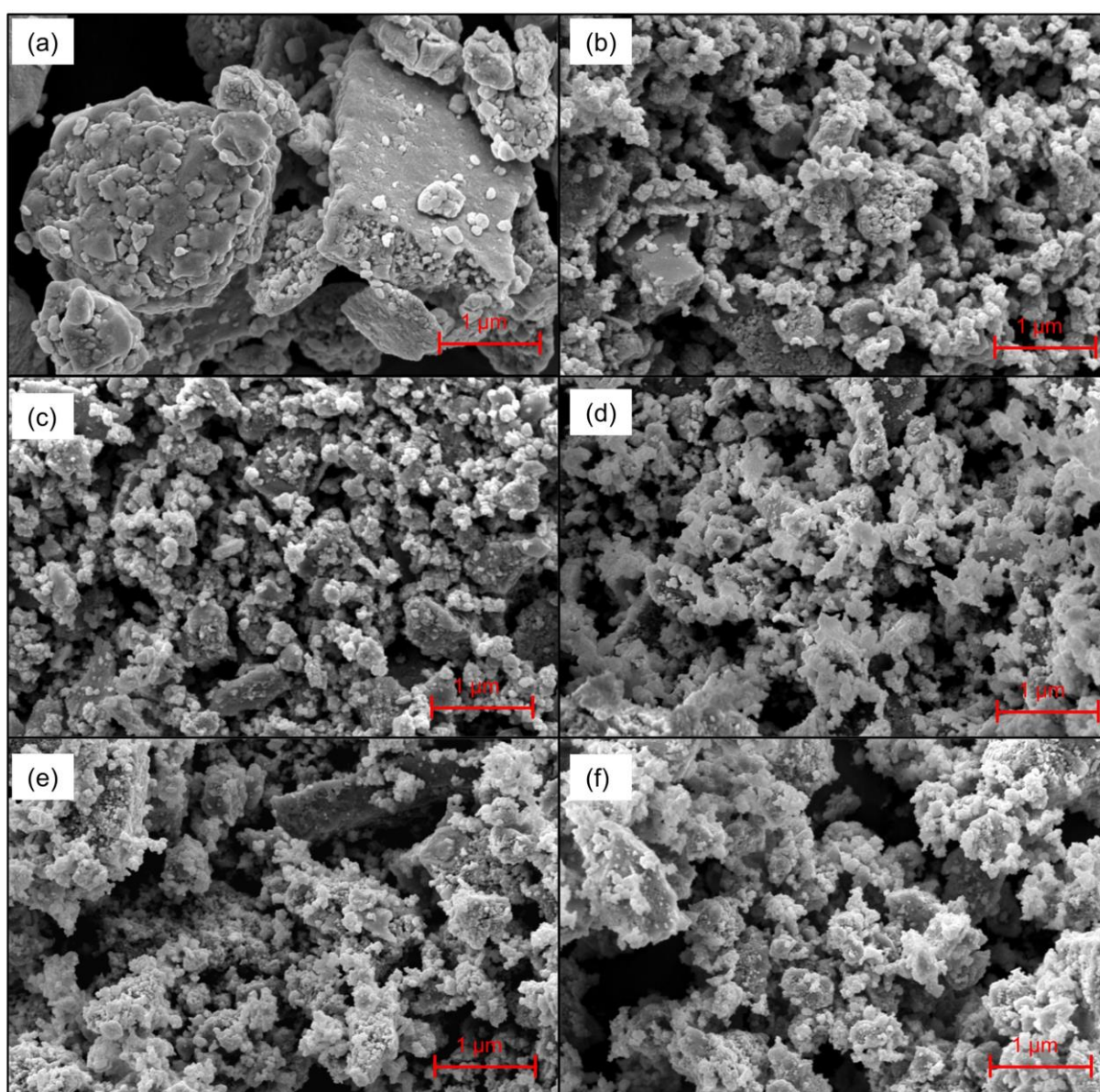


Fig. 9. FESEM images of RP powder and as-prepared BP powders after the ball-milling process using stainless-steel media at 450 rpm varied by milling time; (a) 0 min, (b) 1 h, (c) 2 h, (d) 3 h, (e) 4 h and (f) 5 h

4. Conclusions

The complete transformation of RP into pure BP powder can be obtained via the high energy ball-milling method using stainless steel media and 5 h milling time. Combination of these parameters produced crystalline and orthorhombic structure of BP with aggregated layers microstructure.

Acknowledgement

The study is funded by Ministry of Higher Education (MOHE) of Malaysia through the Fundamental Research Grant Scheme (FRGS) No: FRGS/1/2022/TK09/UTEM/02/59. The Authors also like to thank Universiti Teknikal Malaysia Melaka (UTeM) for all the supports.

References

- [1] Xia, Fengnian, Han Wang, and Yichen Jia. "Rediscovering black phosphorus as an anisotropic layered material for optoelectronics and electronics." *Nature communications* 5, no. 1 (2014): 4458. <https://doi.org/10.1038/ncomms5458>
- [2] Lin, Shenghuang, Yanyong Li, Jiasheng Qian, and Shu Ping Lau. "Emerging opportunities for black phosphorus in energy applications." *Materials Today Energy* 12 (2019): 1-25. <https://doi.org/10.1016/j.mtener.2018.12.004>
- [3] Dinh, Khang Ngoc, Yu Zhang, and Wenping Sun. "The synthesis of black phosphorus: From zero-to three-dimensional nanostructures." *Journal of Physics: Energy* 3, no. 3 (2021): 032007. <https://doi.org/10.1088/2515-7655/abf2da>
- [4] Park, Cheol-Min, and Hun-Joon Sohn. "Black phosphorus and its composite for lithium rechargeable batteries." *Advanced Materials (Weinheim)* 19 (2007). <https://doi.org/10.1002/adma.200602592>
- [5] Suryanarayana, Cury. "Mechanical alloying and milling." *Progress in materials science* 46, no. 1-2 (2001): 1-184. [https://doi.org/10.1016/S0079-6425\(99\)00010-9](https://doi.org/10.1016/S0079-6425(99)00010-9)
- [6] Leonardi, Marco, Mercedes Villacampa, and J. Carlos Menéndez. "Multicomponent mechanochemical synthesis." *Chemical Science* 9, no. 8 (2018): 2042-2064. <https://doi.org/10.1039/C7SC05370C>
- [7] Balasubramanian, Janani, Jack Lemere, S. Sudheer Khan, and Nisha Rani Agarwal. "Plasmonic nanosensors and their spectroscopic applications—current trends and future perspectives." In *Molecular and laser spectroscopy*, pp. 337-372. Elsevier, 2022. <https://doi.org/10.1016/B978-0-323-91249-5.00001-6>
- [8] Zhou, Fengchen, Liuzhang Ouyang, Meiqin Zeng, Jiangwen Liu, Hui Wang, Huaiyu Shao, and Min Zhu. "Growth mechanism of black phosphorus synthesized by different ball milling techniques." *Journal of Alloys and Compounds* 784 (2019): 339-346. <https://doi.org/10.1016/j.jallcom.2019.01.023>
- [9] Shin, Hosop, Jianyu Zhang, and Wei Lu. "A comprehensive study of black phosphorus-graphite composite anodes and HEMM synthesis conditions for improved cycle stability." *Journal of The Electrochemical Society* 166, no. 12 (2019): A2673. <https://doi.org/10.1149/2.1421912jes>
- [10] Chenje, T. W., D. J. Simbi, and E. Navara. "Relationship between microstructure, hardness, impact toughness and wear performance of selected grinding media for mineral ore milling operations." *Materials & design* 25, no. 1 (2004): 11-18. [https://doi.org/10.1016/S0261-3069\(03\)00168-7](https://doi.org/10.1016/S0261-3069(03)00168-7)
- [11] Bao, Ta Na, Ojin Tegus, Hasichaolu Hasichaolu, Ning Jun, and Narengerile Narengerile. "Preparation of black phosphorus by the mechanical ball milling method and its characterization." *Solid State Phenomena* 271 (2018): 18-22. <https://doi.org/10.4028/www.scientific.net/SSP.271.18>
- [12] Pedersen, Samuel V., Florent Muramutsa, Joshua D. Wood, Chad Husko, David Estrada, and Brian J. Jaques. "Mechanochemical conversion kinetics of red to black phosphorus and scaling parameters for high volume synthesis." *npj 2D Materials and Applications* 4, no. 1 (2020): 36. <https://doi.org/10.1038/s41699-020-00170-4>
- [13] Lin, Cheng, Lingli Yang, Liuzhang Ouyang, Jiangwen Liu, Hui Wang, and Min Zhu. "A new method for few-layer graphene preparation via plasma-assisted ball milling." *Journal of Alloys and Compounds* 728 (2017): 578-584. <https://doi.org/10.1016/j.jallcom.2017.09.056>
- [14] Murthy, Bharath Vedashantha, Virupaxi Auradi, Madeva Nagaral, Manjunath Vatnalmath, Nagaraj Namdev, Chandrashekar Anjinappa, Shanawaz Patil et al. "Al₂O₃-alumina aerospace composites: particle size impacts on microstructure, mechanical, fractography, and wear characteristics." *ACS omega* 8, no. 14 (2023): 13444-13455. <https://doi.org/10.1021/acsomega.3c01163>
- [15] Adewuyi, Sefiu O., Hussin AM Ahmed, and Haitham MA Ahmed. "Methods of ore pretreatment for comminution energy reduction." *Minerals* 10, no. 5 (2020): 423. <https://doi.org/10.3390/min10050423>

- [16] Tonello, Maurício Sonda, Jackson Korchagin, and Edson Campanhola Bortoluzzi. "Environmental agate mining impacts and potential use of agate residue in rangeland." *Journal of cleaner production* 280 (2021): 124263. <https://doi.org/10.1016/j.jclepro.2020.124263>
- [17] Zhu, Xianjun, Taiming Zhang, Daochuan Jiang, Hengli Duan, Zijun Sun, Mengmeng Zhang, Hongchang Jin et al. "Stabilizing black phosphorus nanosheets via edge-selective bonding of sacrificial C60 molecules." *Nature Communications* 9, no. 1 (2018): 4177. <https://doi.org/10.1038/s41467-018-06437-1>
- [18] Zhu, JiPing, GuangShun Xiao, and XiuXiu Zuo. "Two-dimensional black phosphorus: an emerging anode material for lithium-ion batteries." *Nano-Micro Letters* 12 (2020): 1-25. <https://doi.org/10.1007/s40820-020-00453-x>
- [19] Gupta, Satyendra Nath, Anjali Singh, Koushik Pal, Biswanath Chakraborti, D. V. S. Muthu, U. V. Waghmare, and A. K. Sood. "Raman anomalies as signatures of pressure induced electronic topological and structural transitions in black phosphorus: Experiments and theory." *Physical Review B* 96, no. 9 (2017): 094104. <https://doi.org/10.1103/PhysRevB.96.094104>
- [20] Liu, Yue, Jiaxin Zou, Shurui Chen, Bo Zhong, Yingying Wang, Huatao Wang, and Xiaoxiao Huang. "Raman spectroscopy studies of black phosphorus." *Spectrochimica Acta Part A: Molecular and Biomolecular Spectroscopy* 271 (2022): 120861. <https://doi.org/10.1016/j.saa.2022.120861>
- [21] Cui, Li, Holly J. Butler, Pierre L. Martin-Hirsch, and Francis L. Martin. "Aluminium foil as a potential substrate for ATR-FTIR, transfection FTIR or Raman spectrochemical analysis of biological specimens." *Analytical methods* 8, no. 3 (2016): 481-487. <https://doi.org/10.1039/C5AY02638E>
- [22] Mogensen, Klaus Bo, Marina Gühlke, Janina Kneipp, Shima Kadkhodazadeh, Jakob B. Wagner, Marta Espina Palanco, Harald Kneipp, and Katrin Kneipp. "Surface-enhanced Raman scattering on aluminum using near infrared and visible excitation." *Chemical communications* 50, no. 28 (2014): 3744-3746. <https://doi.org/10.1039/C4CC00010B>
- [23] Kou, Liangzhi, Changfeng Chen, and Sean C. Smith. "Phosphorene: fabrication, properties, and applications." *The journal of physical chemistry letters* 6, no. 14 (2015): 2794-2805. <https://doi.org/10.1021/acs.jpcllett.5b01094>
- [24] Frisenda, Riccardo, Yue Niu, Patricia Gant, Manuel Muñoz, and Andres Castellanos-Gomez. "Naturally occurring van der Waals materials." *npj 2D Materials and Applications* 4, no. 1 (2020): 38. <https://doi.org/10.1038/s41699-020-00172-2>
- [25] Gao, Ping, Yufen Xiao, Yuliang Wang, Leijiao Li, Wenliang Li, and Wei Tao. "Biomedical applications of 2D mono-elemental materials formed by group VA and VIA: a concise review." *Journal of Nanobiotechnology* 19 (2021): 1-23. <https://doi.org/10.1186/s12951-021-00825-4>
- [26] Xue, Xiong-Xiong, Haiyu Meng, Zongyu Huang, Yexin Feng, and Xiang Qi. "Black phosphorus-based materials for energy storage and electrocatalytic applications." *Journal of Physics: Energy* 3, no. 4 (2021): 042002. <https://doi.org/10.1088/2515-7655/abff6b>
- [27] Gou, Jihua, Jinfeng Zhuge, and Fei Liang. "Processing of polymer nanocomposites." In *Manufacturing Techniques for Polymer Matrix Composites (PMCs)*, pp. 95-119. Woodhead Publishing, 2012. <https://doi.org/10.1533/9780857096258.1.95>
- [28] Wang, Wei, Guoxin Xie, and Jianbin Luo. "Black phosphorus as a new lubricant." *Friction* 6 (2018): 116-142. <https://doi.org/10.1007/s40544-018-0204-z>
- [29] Liu, Jie, Shunhong Zhang, Yaguang Guo, and Qian Wang. "Phosphorus K 4 Crystal: A New Stable Allotrope." *Scientific Reports* 6, no. 1 (2016): 37528. <https://doi.org/10.1038/srep37528>